Desalination and Water Treatment
www.deswater.com

doi: 10.5004/dwt.2017.20136

62 (2017) 449–456
February

Kinetic and thermodynamic study of nitrate adsorption from aqueous solution by lignocellulose-based anion resins

Muhammad Tariq Bashir*, Salmiaton Ali, Azni Idris, Razif Harun

Department of Chemical and Environmental Engineering, Universiti Putra Malaysia, Serdang, Selangor, Malaysia, emails: engrmtb@hotmail.com (M.T. Bashir), mie@upm.edu.my (A. Salmiaton), azni@upm.edu.my (A. Idris), razif@upm.edu.my (R. Harun)

Received 7 April 2016; Accepted 7 August 2016

ABSTRACT

Nitrates are present in drinking water sources and pose serious health issues in many countries throughout the world. In this research, nitrate removal by palm kernel shell-based lignocellulose anion resins was studied under various nitrate concentrations, pH, and adsorbent dosages. The nitrate adsorption capacity demonstrated by the biomaterial-based resins was 53.18 mg/L. A pseudo-second order model and the Weber–Morris diffusion model were used to assess the adsorption process. The thermodynamic study predicted the exothermic nature of the process and the dominance of physical adsorption. Resins were characterized using elemental, proximate, and chemical analyses as well as by the pH at the point of zero charge. The lignocellulose-based adsorbent is a satisfactory material for nitrate removal from water and can be regenerated and reused.

Keywords: Adsorption; Nitrate; Palm kernel shell; Reaction kinetics; Thermodynamics

1. Introduction

Nitrate contamination in natural water resources has emerged as a global issue in the last few decades [1,2]. Elevated concentrations of nitrate in drinking water (i.e., >10 ppm as nitrogen or >45 mg/L as the ion), may cause methemoglobinemia in infants [3,4]. Miscarriages in pregnant women have also been reported due to nitrate toxicity. The long-term effects of nitrate in drinking water include esophageal and gastric cancer (due to the bonding of the amines and amides with nitrite), hypertension, breast shortening, and hemorrhaging of the spleen. [3,5]. High concentrations of nitrate in drinking water and animal feed can result in reduced vitality and an increase in still births, low birth weight or even death in animals [6]. Despite these health risks, the nitrate concentration in drinking water is as high as 200 ppm in a large number of countries, including Pakistan, India, Nepal, Sri Lanka, Nigeria China, Mexico, and Canada [1,7].

Many technologies for nitrate removal from water exist and are based on ion exchange [8], membrane filtration [9], and chemical and biological methods [10,11]. Unsurprisingly, many of these technologies are expensive or complex and are not suitable for application in low-income and developing countries. Adsorption-based techniques are deemed to be the most suitable technology for such countries. Furthermore, adsorbents prepared from agricultural wastes using chemical processes are considered to be eco-friendly and economical.

Many anion exchangers are produced by grafting lignocellulosic agricultural wastes with amine groups. Orlando et al. [12] transformed agro-waste into an anion exchanger by grafting a variety of agricultural wastes including sawdust, rice husk, pine bark, sugarcane bagasse, *Moringa oleifera* hull, coconut husk and persimmon tea leaf. To create the exchanger, Orlando et al. [12] employed a chain reaction of epichlorohydrin and dimethylamine using pyridine as a catalyst (EDM method). Keränen et al. [13] also prepared adsorbent using the EDM method for nitrate removal using pine sawdust and bark. Diriba et al. [14] and Xu et al. [15] also developed wheat straw-based anion exchangers for effective removal of nitrate

* Corresponding author.

from aqueous solutions. Palm kernel shell can also be modified to enhance its affinity for the removal of anions [16,17].

In this research, lignocellulose-based anion resins were prepared using palm kernel shells (PKS) as a precursor; PKS is an agricultural waste generated in the processing of palm oil. The study particularly provided an insight into the lignocellulosic contents derived from PKS and its suitability for nitrate removal, as well as the kinetic behavior and thermodynamics of adsorption.

2. Materials and methods

2.1. Materials and sample solution

The chemicals used were potassium nitrate (KNO_3), N-(3 Chloro-2 Hydroxypropyl) Trimethylammonium Chloride (CHMAC), and potassium hydroxide (KOH pellets). All were of analytical grade (Sigma–Aldrich, Germany) and were used without further purification. The nitrate stock solution was prepared by mixing 1.63 g of KNO_3 in 1 L of deionized water (Milli-Q Water). Solutions of the required nitrate concentrations in a range 25–225 mg/L (25, 50, 75, 100, 125, 150, 175, 200 and 225 mg/L) were obtained by diluting the nitrate stock solution.

2.2. Chemical modification of the palm kernel shell

The PKS-based lignocellulosic content was used to prepare anion resins (PKS-AR). The ground PKS was mercerized by treating it with potassium hydroxide as reported in our previous research for fluoride adsorption [16]. The mercerized particles were reacted in a mixture of 5 M KOH and CHMAC (1:1.5 v/v) for quaternization. The dried resins were sieved to obtain a particle size of 0.25–0.5 mm for subsequent use.

2.3. Characterization of PKS and PKS-AR

An elemental analyzer (Perkin Elmer- Series II 2400, Japan) was used to determine the elemental constituents (hydrogen, nitrogen, carbon, and sulfur) of the PKS, PKS-AR and nitrate-loaded PKS-AR. Thermogravimetric analysis (TGA) equipment (Model Perkin Elmer TGA7, USA) was used in the proximate and chemical analysis of PKS and PKS-AR samples. The pH at the point of zero charge (pHpzc) of PKS-AR was determined using the pH drift method. The drift method involved placing a 0.3-g sample of adsorbent in each of eight Erlenmeyer flasks containing 100 ml of 0.01 M NaCl solution. The acidity was calibrated in the range of pH 2–10 (± 0.2) using 0.1 M NaOH and 0.1 M HCl. The sealed flasks were agitated in an incubator shaker at 120 rpm for 48 h.

2.4. Static study

Batch experiments were conducted at 28°C to investigate the influence of absorbent dose (at pH 6), initial nitrate concentration (25–225 mg/L) at pH 6 and pH 7 and contact times at pH 6 and pH 7. The static study was also conducted at 20°C, 30°C and 40°C to determine the thermodynamics of adsorption (at initial nitrate concentration: 25–225 mg/L). A nitrate solution with a concentration of 25 mg/L was selected to define all other requisite parameters.

2.5. Isotherm modelling

Langmuir and Freundlich isotherm models were employed to assess adsorption data at pH 6 and pH 7. The linearized form of the Langmuir model (Eq. (1)) was used [18].

$$\frac{1}{q_e} = \frac{1}{Q_L * b * C_e} + \frac{1}{Q_L} \tag{1}$$

The linearized form of the Freundlich isotherm model (Eq. 2) was also employed to investigate the adsorption data.

$$\log q_e = \log K_f + \frac{1}{n}\log C_e \tag{2}$$

In Eqs. (1) and (2), C_e is the equilibrium concentration (mg/L); q_e and Q_L are adsorptions at equilibrium and Langmuir monolayer capacity (mg/g), respectively; '*b*' is the Langmuir isotherm model constant (L/mg); K_f and '*n*' are the Freundlich isotherm constant and adsorbent intensity, respectively in the Freundlich model.

2.6. Kinetic modelling of nitrate adsorption

The kinetic behavior of nitrate removal by PKS-AR was described using pseudo-second order and the Weber-Morris diffusion model. Eqs. (3)–(5) were used for calculating the requisite parameters. Moreover, Eq. (3) can be modified to Eq. (4) for prediction of the initial kinetic rate in the pseudo-second order model [19].

$$\frac{t}{q_t} = \frac{1}{K_1 q_e^{\,2}} + \frac{1}{q_e}t \tag{3}$$

$$\frac{t}{q_t} = \frac{1}{h} + \frac{1}{q_e}t \tag{4}$$

$$q_t = K_{\mathrm{id}} t^{0.5} + C_{\mathrm{id}} \tag{5}$$

In these equations, '*t*' is time (min), K_1 is the pseudo-second order constant (g/mg-min) and $h = (K_2 \times q_e^{\,2})$, which describes the initial uptake rate (g/mg-min). In Eq. (5), K_{id} is the intra-particle diffusion constant (mg/g-min) and C_{id} is the thickness of boundary layers. The parameter K_{id} can be calculated by the slope of the plot of q_t vs. $t^{0.5}$.

2.7. Thermodynamic study of nitrate adsorption

To evaluate the thermodynamics of adsorption, it is imperative to calculate thermodynamic parameters such as the change in free Gibbs energy '$\Delta G°$' (kJ/mol), enthalpy change '$\Delta H°$' (kJ/mol), and entropy change '$\Delta S°$' (kJ/mol K). These parameters can be determined using Eq. (6) and the van't Hoff equation (Eq. (7)).

$$\Delta G° = -RT\ln K \tag{6}$$

$$\ln K = \frac{\Delta S°}{R} - \frac{\Delta H°}{RT} \tag{7}$$

In Eqs. (6) and (7), R is the gas constant (8.314 × 10^{-3} kJ/mol-K) and T is absolute temperature (°K). The equilibrium constant '*K*' relates to the Langmuir constant '*b*' measured in (L/mg) and can be obtained by multiplying '*b*' by a factor of 10^6 [20]. By plotting "ln *K*" against "1/*T*" in the van't Hoff equation, the intercept and slope can be obtained to determine ΔS° and ΔH°, respectively.

3. Results and discussion

3.1. CHN analysis

The Carbon-Hydrogen-Nitrogen (CHN) analysis quantified the proportions of these three elements in raw PKS as 50.59, 5.73 and 3.31 wt%, respectively (Table 1). Moreover, the CHN analysis revealed 80.59% increase of nitrogen by weight in PKS-AR and an additional 14.19% increase in the exhausted PKS-AR after adsorption. These results proved a successful reaction of the functional group and removal of nitrate from the aqueous solution. The percentage of nitrogen that is of prime interest was observed to be sufficiently high in raw PKS and PKS-AR, as predicted by the CHN analysis.

3.2. Thermogravimetric and differential thermal analysis

Thermographs revealed the presence of volatile matter, fixed carbon and ash content in PKS (55.21, 32.49, and 6.93 wt%, respectively) and in PKS-AR (53.58, 29.60 and 7.97 wt%, respectively). In addition, differential thermal analysis (DTA) and TGA thermographs of PKS and chemically modified PKS (PKS-AR) exposed radical changes at different stages, indicating loss of weight due to moisture loss and organic matter loss, followed by decomposition of hemicellulose and cellulose at peak temperatures of 283°C and 360°C, respectively (Table 2). The lignin decomposition in PKS-AR and PKS occurred between 281°C and 521°C, with a peak value at 434°C as well as between 263°C and 480°C, respectively. These changes are associated with numerous oxygen and functional groups present on PKS and PKS-AR that resulted in varying thermal solidities [17,21]. The amount of cellulose, hemicellulose, and lignin in PKS was calculated as 29.85, 24.33, and 49.58 wt%, respectively, whereas in PKS-AR the amount of each compound was 26.26, 19.78, and 37.13 wt%, respectively (Table 2). In fact, the composition of PKS is difficult to predict because the precise composition of cellulose $(C_6H_{10}O_5)_n$, hemicellulose $(C_5H_8O_4)_n$ and lignin in an organic material is hard to predict [21,22].

Table 1
CHN analysis of PKS, PKS-AR and nitrate-loaded PKS-AR

Description	Carbon (wt%)	Hydrogen (wt%)	Nitrogen (wt%)	Sulfur (wt%)	Oxygen (wt%)
Raw PKS	50.59	5.73	3.31	0.0019	4,037
PKS-AR	48.97	6.37	17.06	0.0233	27.58
Nitrate-loaded PKS-AR	49.07	6.45	19.88	0.0169	24.58

Table 2
Chemical composition and proximate analysis of PKS and PKS-AR

Material	PKS	PKS-AR
Cellulose (wt%)	29.85	26.26
Hemicellulose (wt%)	24.33	19.78
Lignin (wt%)	49.58	37.13
Extractives (wt%)	13.25	9.63
Volatile matter (wt%)	55.21	53.58
Fixed carbon (wt%)	32.49	29.60
Ash (wt%)	6.93	7.97
Moisture (wt%)	5.35	8.85

3.3. pH at point of zero charge (pHpzc) of PKS-AR

Using the drift method, the difference in pH (ΔH) was calculated, and a relationship was developed between initial pH and change in pH (Fig. 1). The pH at the point of zero charge (pHpzc) was found to be 7.7, which revealed a positive surface charge density on PKS-AR in the range of pH 2–8 (± 0.2).

3.4. Effect of the initial nitrate concentration and adsorbent dosage

The effect of initial nitrate concentration on nitrate removal efficiency was investigated using 0.4 g of PKS-AR (adsorbent) at a range of initial nitrate concentrations (25–225 mg/L) at pH 6 and pH 7. Fig. 2(A) shows that the nitrate removal efficiency decreased from 79.6% to 62.5% and from 79.24% to 62.15% at pH 6 and pH 7, respectively, when the initial nitrate concentration increased from 25 to 225 mg/L. The amount of adsorbed nitrate increased from 4.98 to 35.16 mg/g and from 4.95 to 34.96 mg/g at pH 6 and pH 7, respectively, at corresponding equilibrium concentrations (Fig. 2(B)) because of the nitrate mass transfer that occurred between the liquid and solid phases [23,24]. A slight difference in efficiency and adsorption was observed at pH 6 and pH 7 due to the high value of pHpzc (7.7), indicating that remarkable adsorption can occur at a wide range of pH.

The effect of adsorbent dosage on nitrate adsorption was further investigated at pH 6. As expected, an increase in the dose of adsorbent resulted in a corresponding increase in nitrate removal of up to 82.3% (at a dosage of 4 g /L) (Fig. 3). Further increases of the dose (beyond 0.4 g) resulted in only a slight increase in nitrate removal (to 84.04%). This trend

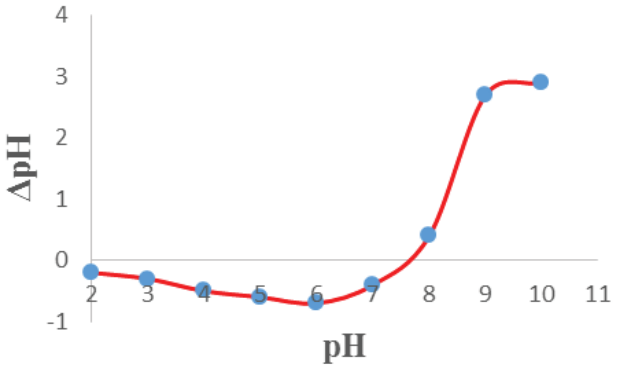

Fig. 1. Plot of pH vs. ΔpH for point of zero charge on PKS-AR (the adsorbent).

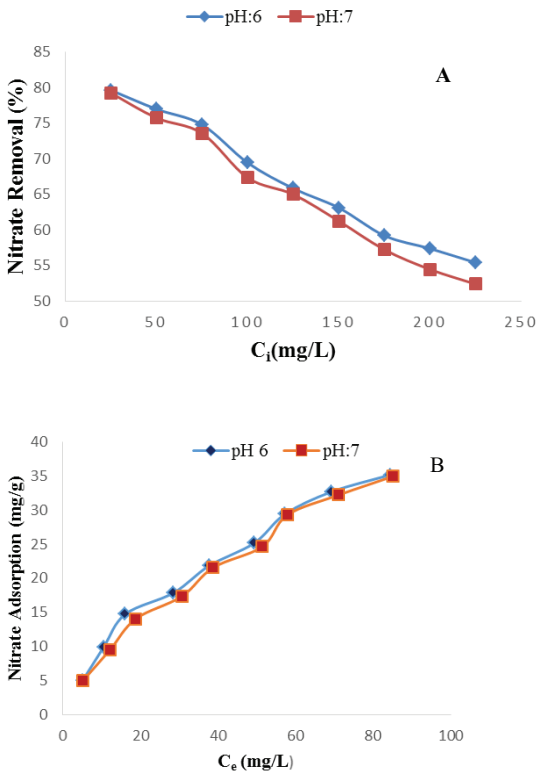

Fig. 2. Effect of initial nitrate concentration (C_i) at pH 6 and pH 7 on nitrate adsorption by palm kernel shell anion resins (PKS-AR) adsorbent (A), and equilibrium concentration on nitrate adsorption capacity (mg/g) of PKS-AR (B). (Dosage of adsorbent was 4 g/L).

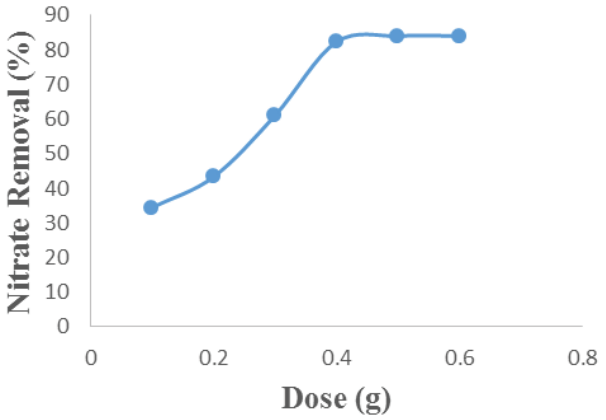

Fig. 3. Nitrate removal at different doses of PKS-AR adsorbent (nitrate concentration: 25 mg/L and pH: 6).

occurred due to the coincidence of dynamic sites and is analogous to results reported for other chemically modified biomaterials, such as wheat straw, sawdust, and rice husk [15,24].

3.5. Langmuir and Freundlich isotherm analysis

Langmuir and Freundlich isotherms were used to assess data obtained in static studies for nitrate removal. The value

Table 3
Langmuir and Freundlich parameters for describing nitrate adsorption on PKS-AR

Isotherm	pH	Parameters	Nitrate Adsorption
Langmuir	6	Q_0 (mg/g)	53.12
		b (L/mg)	0.0204
		R^2	0.994
Langmuir	7	Q_0 (mg/g)	51.81
		b (L/mg)	0.0203
		R^2	0.996
Freundlich	6	K_f (mg/g)	1.833
		$1/n$	0.68
		n	1.471
		R^2	0.982
Freundlich	7	K_f (mg/g)	1.708
		$1/n$	0.697
		n	1.435
		R^2	0.985

for the separation factor 'R_L' resulting from the application of the Langmuir isotherm model (R_L < 1) suggested that nitrate removal by PKS-AR occurred by monolayer adsorption. On the other hand, the acquired values of '1/n' in the Freundlich isotherm were observed to be between 0 and 1, which indicated the limited applicability of a multilayer adsorption model. Moreover, the correlation coefficients between measured nitrate adsorption and adsorption predicted by the Langmuir isotherm were close to unity at both values of pH (R^2 = 0.994 at pH 6 and R^2 = 0.996 at pH 7) (Table 3). In addition, in the plots of q_e vs. C_e the Langmuir isotherm described the removal of nitrate slight better than the Freundlich isotherm, which is an indication of the dominance of the monolayers (Figs. 4(A) and (B)). The maximum nitrate adsorption capacity of PKS-AR predicted by the Langmuir isotherm was 53.12 and 51.81 mg/g at pH 6 and pH 7, respectively. In previous research, the adsorption of nitrate on cellulose-based adsorbent was also reported to follow the Langmuir isotherm; these materials included almond shell [25], wheat straw [15], coconut coir pith [26], and birch bark [13].

3.6. Kinetic behavior of nitrate adsorption

The kinetics of nitrate removal were investigated at initial nitrate concentrations (25, 50 and 100 mg/L) at constant adsorbent dose (4 g/L) and pH 6. The kinetic was also accessed at constant nitrate concentration (25 mg/L) at pH 7. Maximum adsorption was observed to occur within 5 min at both values of pH (initial nitrate concentration: 25 mg/L). Equilibrium was attained after 30 min with a nitrate removal efficiency of 79.1% and 78.6% at pH 6 and pH 7, respectively (Fig. 5). To define the kinetic behavior of nitrate removal, the experimental data were fitted to pseudo-second order model and the Weber-Morris model. The pseudo-second order model provided a good agreement in the description of the nitrate adsorption kinetics (Fig. 6 and Table 4). The rate constant of the pseudo-second

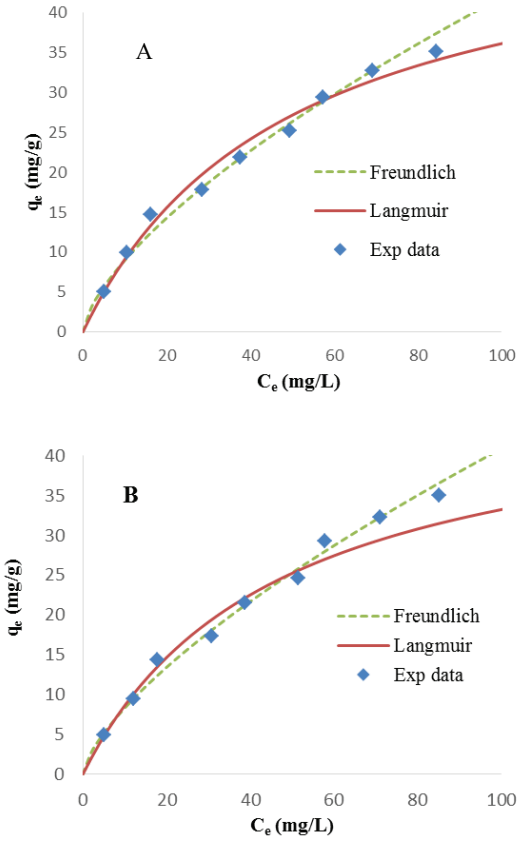

Fig. 4. Langmuir and Freundlich adsorption isotherms for nitrate removal (q_e) by PKS-AR at pH 6 (A) and pH 7 (B) as a function of equilibrium nitrate concentration (C_e). (The adsorbent dosage was 4 g/L).

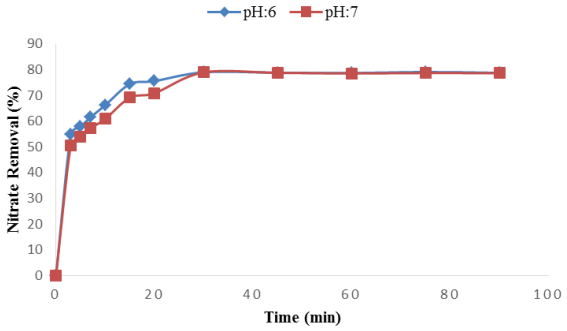

Fig. 5. Nitrate removal (%) vs. time (min) at pH 6 and pH 7 (Initial nitrate concentration was 25 mg/L and the PKS-AR dose was 4 g/L).

order model decreased from 0.0967 to 0.0674 g/mg-min as the pH increased from 6 to 7. This result occurred because of the higher availability of OH^- on PKS-AR at pH 7 than at pH 6. On the other hand, rate constant decreased from 0.0967 to 0.0192 g/mg-min when concentration increased from 25 to 100 mg/L. Moreover, the value of the initial rate constant (h) was found to be 2.603, 3.074 and 6.452 mg/g-min at corresponding nitrate concentrations (25, 50 and 100 mg/L), respectively (Table 4).

One of the main characteristics of the solute-transfer process in solid-liquid adsorption is that of external mass transfer, which can also be understood as boundary diffusion [27]. The rate-limiting step in the adsorption of nitrate by resins was investigated by plotting the amount of nitrate adsorbed against the square root of time, based on the Weber-Morris model (Figs. 7(A) and (B)). The values of K_{id} were found to be 3.61×10^{-2} mg/g-min, 4.41×10^{-2} mg/g-min and 8.63×10^{-2} mg/g-min when nitrate was exposed to PKS-AR at nitrate concentration (25, 50 and 100 mg/L, respectively and at pH 6) as well as 4.88×10^{-2} mg/g-min at pH 7 (at nitrate concentration: 25 mg/L). The variable rate of nitrate adsorption on PKS-AR is visible in Figs. 7(A) and (B), which highlights an initial phase influenced by boundary layer diffusion, a second phase controlled by intra-particle diffusion, and a final phase that reflected an equilibrium stage. The fact is that neither curve passes through the origin indicates that the process of nitrate removal on PKS-AR is rather complex and affected by both the intra-particle diffusion and by surface adsorption [24,28].

3.7. Thermodynamics of adsorption

The van't Hoff equation (Eq. 8) was used to plot 'ln K' vs. '1/T' resulting in a correlation coefficient (R^2) of 0.99 (Fig. 8). The values of ΔG° for nitrate were calculated as –24.59 kJ/mol (at 20°C), –25.36 kJ/mol (at 30°C) and –26.13 kJ/mol (at 40°C) (Table 5). The standard Gibbs free energy (which describes the spontaneity of the nitrate sorption process) has a negative value at all the temperatures examined in this study. Moreover, the nature of the interaction of nitrate with PKS-AR was found to be exothermic, as indicated by the negative value of 'ΔH°' (–2.05 kJ/mol). Because the change in enthalpy was less than 40 KJ/mol, the adsorption process was predominantly physical in nature and possibly occurred by surface adsorption [29] despite the slight degree of ion exchange or chemisorption [30]. Also, the change in standard entropy for the adsorption process was positive (Table 5) illustrating that the nitrate anion (NO_3^{-1}) has an increasing degree of freedom [20,31].

Table 4
Summary of parameters for a pseudo-second order kinetic model and the Weber-Morris model to describe nitrate adsorption

pH	C_i mg/L	q_e (Exp.) mg/g	Pseudo-Second Order Model			h (mg/g-min)	Weber-Morris Model		
			K_2 (g/mg-min)	q_e (mg/g)	R^2		K_{id} (mg/g-min)	C_{id}	R^2
6	25	4.993	0.0967	5.189	0.999	2.603	3.61×10^{-2}	3.17	0.826
6	50	9.62	0.0287	10.352	0.995	3.074	10.93×10^{-2}	4.41	0.619
6	100	17.2	0.0192	18.315	0.995	6.452	18.18×10^{-2}	8.63	0.565
7	25	4.94	0.0674	5.206	0.998	1.827	4.88×10^{-2}	3.59	0.791

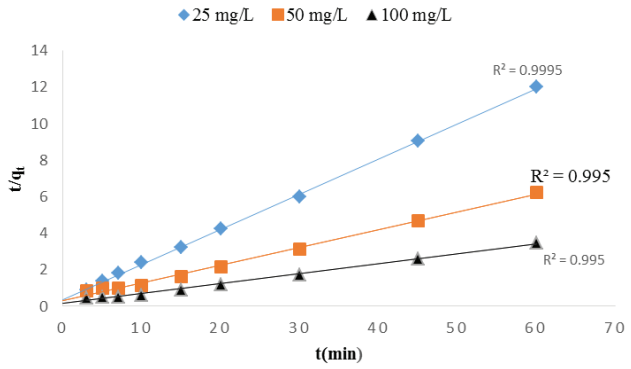

Fig. 6. Representation by a pseudo-second-order model of nitrate adsorption (t/q_t) by PKS-AR at different initial concentrations (pH: 6, dosage: 4 g/L).

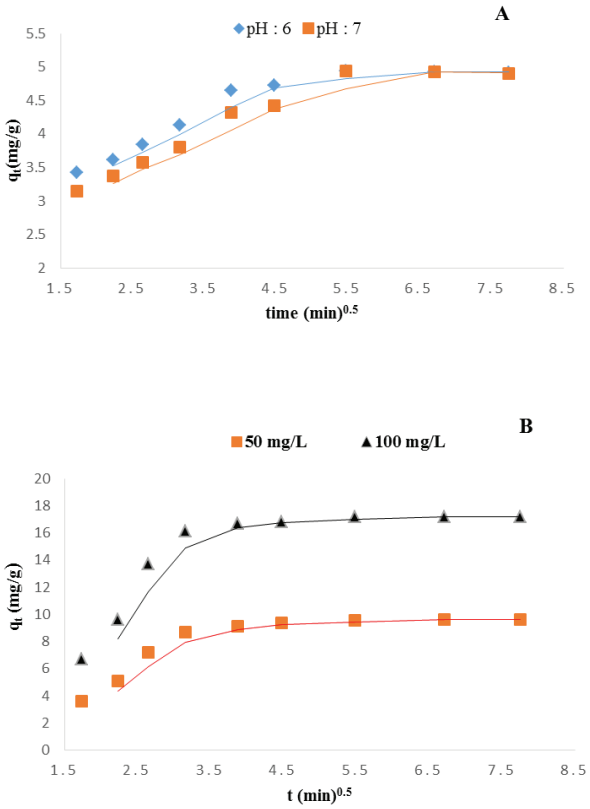

Fig. 7. Amount of nitrate adsorbed (q_t) on PKS-AR vs. square root of time, highlighting the effect of intra-particle diffusion (nitrate concentration: 25 mg/L at pH 6 and pH 7 and PKS-AR dosage: 4 g/L) (A) and at different nitrate concentrations (pH: 6, PKS-AR dosage: 4 g/L) (B).

3.8. Regeneration and reuse of the PKS-AR

With regard to the economical application of anion adsorption, an adsorbent should be suitable for regeneration and reuse. Regeneration and reuse of the adsorbent also facilitates waste minimization. This study employed 0.1 M NaCl as an eluent to regenerate the PKS-AR, based on the economy and eco-friendly options for disposal of generated waste. In the second and third operation cycles, the PKS-AR adsorbent removed 84% of the influent nitrate, which was better performance than was achieved using fresh adsorbent. The resins also showed remarkable results in subsequent cycles, removing 97% of first cycle for influent nitrate in the fifth consecutive cycle (Fig. 9). This efficacy demonstrated a strong ion exchange reaction during the regeneration process, which could be ascribed to partial displacement of NO_3^{-1} with Cl^{-1} as well as the reaction of sodium with nitrate (which displaced the adsorbed nitrate completely). In addition, the regeneration process may have removed possible impurities present in the resins as well as reduced the concentration of OH^{-1} ions. Consequently, regeneration increased the number of active sites that were positively charged, improving the removal of nitrate through approximately three initial operation-regeneration cycles.

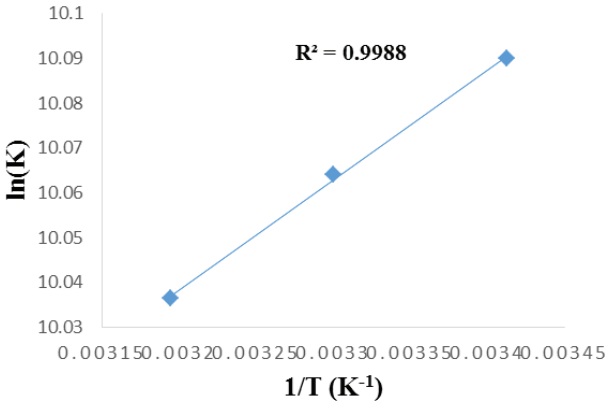

Fig. 8. van't Hoff plot of $1/T$ vs. $\ln(K)$ for nitrate adsorption on PKS-AR.

3.9. Column study

Two nitrate concentrations (50 and 100 mg/L) were studied using column analysis (at a flow rate of 7 ml/min and a column diameter of 11 mm). The breakthrough point was ascertained by plotting the ratio of influent nitrate concentration to effluent concentration (C_t/C_i) vs. time, as described in the literature [13]. In this study, the breakthrough time of the 100 mg/L solution was observed to be much shorter than that for the 50 mg/L solution, a trend that also has been reported in previous column studies using chemically modified biomaterials [13,32]. This column study further confirmed the effectiveness of the adsorbent in removing nitrate from aqueous solutions, showing adsorption capacities to be 28.69 and 47.97 mg/g when treating solutions containing 50 and 100 mg/L nitrate, respectively (Fig. 10).

3.10. Comparison with other biadsorbents

Nitrate removal using other adsorbents reported in previous studies has been compared with this research (Table 6) and PKS-AR was found better than many other adsorbents.

Table 5
Thermodynamic parameters for adsorption of nitrate on PKS-AR

Temperature (°C)	Q (mg/g)	b (L/mg)	K	ΔG° (kJ/mol)	ΔH° (kJ/mol)	ΔS° (kJ/(mol-K)
20	60.77	0.0241	2,4101.4	–24.59	–2.05	0.077
30	49.32	0.0235	2,3480.9	–25.36	–2.05	
40	45.61	0.0228	2,2841.8	–26.13	–2.05	

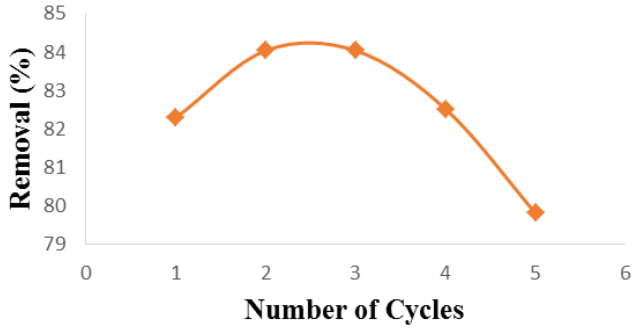

Fig. 9. Nitrate removal (%) by regenerated PKS-AR as a function of operation-regeneration cycles.

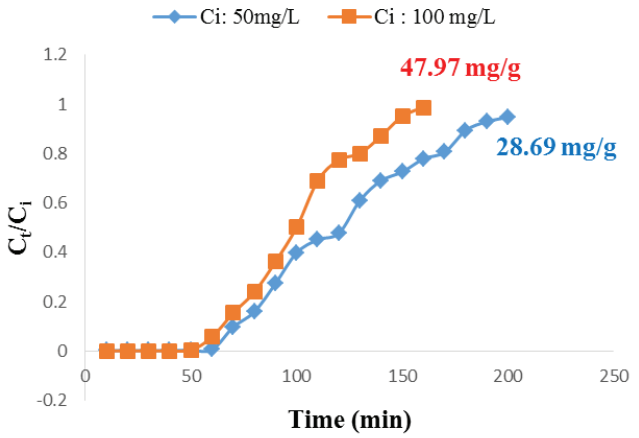

Fig. 10. Breakthrough curves for nitrate adsorption in a fixed bed column with initial nitrate concentrations (C_i) of 100 and 50 mg/L at flow rate of 7 ml/min.

4. Conclusions

Biomaterial-based anion exchange resins (PKS-AR) were successfully prepared by the mercerization of the palm kernel shell, with subsequent quaternization using CHMAC. The Langmuir and Freundlich isotherm models successfully described nitrate adsorption on PKS-AR, although the Langmuir model (R^2 = 0.994) did so slightly better than the Freundlich model (R^2 = 0.982). The adsorption capacity of PKS-AR was determined to be 53.12 mg/g. A pseudo-second order model was found to well explain the kinetic phenomena of the nitrate adsorption process. Thermodynamic analysis of the adsorption process revealed the exothermic behavior and physical nature of the process. The PKS-AR adsorbent can be repeatedly used over a number of operation-regeneration cycles, with only a nominal decrease in nitrate removal efficiency. Column analysis showed the adsorbent has a nitrate removal capacity of 47.97 mg/g, making the material an eco-friendly and feasible adsorbent.

Table 6
Overview of efficacy and comparison of reported bioadsorbents prepared by surface modification for nitrate removal

Bioadsorbents	pH	Conc. Range (mg/L)	Adsorption capacity (mg/g)	Reference
PKS-AR	6	25–225	53.12	This study
PKS-AR	7	25–225	51.81	This study
Almond shell	6.2	10–50	16	[25]
Wheat straw	6	50–500	52.8	[15]
Arundo Donax L. Reed	–	–	44.6	[33]
Chitosan	5	25–1,000	104	[34]
Coconut coir pith	3	10–40	10.3	[26]
Sugar beet bagasse	6.58	300	9.14	[35]
Pine sawdust	5.3–6.4	5–350[a]	30.1[a]	[13]
Mod. spruce bark	5.3–6.4	5–350[a]	26.5[a]	[13]
Coconut husk	6.5	1–30	0.89[b]	[12]
Rice husk	6.5	1–30	1.20[b]	[12]
Coconut granulated AC	6.0–6.4	5–200	10.2	[29]

[a]Concentration as N.
[b]mmol/g.

References

[1] A. Azizullah, M. Khattak, P. Richter, D. Haider, Water pollution in Pakistan and its impact on public health: a review, Environ. Int., 37 (2011) 479–497.
[2] B. Gu, Y. Ge, S. Chang, W. Luo, J. Chang, Nitrate in groundwater of China: sources and driving forces, Glob. Environ. Change, 23 (2013) 1112–1121.
[3] C. Yang, D. Wu, C. Chang, Nitrate in drinking water and risk of death from colon cancer in Taiwan, Environ. Int., 33 (2007) 649–653.
[4] EPA, Drinking Water Standards and Health Advisories EPA 820-R-11-002, U.S. Environmental Protection Agency, Washington, DC, 2011. Available online at: http://water.epa.gov/action/advisories/drinking/upload/dwstandards2011.pdf
[5] S. Mahmood, N. Taj, F. Parveen, T. Usmani, R. Azmat, F. Uddin, Arsenic, fluoride and nitrate in drinking water: the problem and its possible solution, Res. J. Environ. Sci., 1 (2007) 179–184.
[6] I. Dar, M. Dar, K. Sankar, Nitrate contamination in groundwater of Sopore town and its environs, Kashmir, India, Arab J. Geosci., 3 (2009) 267–272.
[7] WHO, Water Quality and Health Strategy 2013–2020. World Health Organisation, Geneva, 2013. Available online at: http://www.who.int/water_sanitation_health/publications/2013/water_quality_strategy/en/

[8] P. Loganathan, S. Vigneswaran, J. Kandasamy, J. Enhanced removal of nitrate from water using surface modification of adsorbents- A review, J. Environ. Manage., 131 (2013) 363–374.
[9] J. Schoeman, Nitrate-nitrogen removal with small-scale reverse osmosis, electrodialysis and ion-exchange units in rural areas, Afr. J., 35 (2009) 721–728.
[10] A. Bhatnagar, M. Sillanpää, A review of emerging adsorbents for nitrate removal from water, Chem. Eng. J., 168 (2011) 493–504.
[11] M. Kumar, S. Chakraborty, Chemical denitrification of water by zero-valent magnesium powder, J. Hazard. Mater., 135 (2006) 112–121.
[12] U. Orlando, A. Baes, W. Nishijima, M. Okada, Preparation of agricultural residue anion exchangers and its nitrate maximum adsorption capacity, Chemosphere, 48 (2002) 1041–1046.
[13] A. Keränen, T. Leiviskä, B. Gao, O. Hormi, J. Tanskanen, Preparation of novel anion exchangers from pine sawdust and bark, spruce bark, birch bark and peat for the removal of nitrate, Chem. Eng. Sci., 98 (2013) 59–68.
[14] D. Diriba, A. Hussen, V. Rao, Removal of nitrite from aqueous solution using sugarcane bagasse and wheat straw, Bull. Environ. Contam. Toxicol., 93 (2014) 126–131.
[15] X. Xu, B. Gao, Q. Yue, Q. Zhong, Preparation of agricultural by-product based anion exchanger and its utilization for nitrate and phosphate removal, Bioresour. Technol., 101 (2010) 8558–8564.
[16] M.T. Bashir, A. Salmiaton, I. Azni, M.M. Nourouzi, R. Harun, Fluoride removal by chemical modification of palm kernel shell-based adsorbent: a novel agricultural waste utilization approach, Asian J. Microbiol. Biotechnol. Environ. Sci., 17 (2015) 533–542.
[17] Y. Koay, I. Ahamad, M. Nourouzi, L. Abdullah, T. Choong, Development of novel low-cost quaternized adsorbent from palm oil agriculture waste for reactive dye removal, Bioresources, 9 (2014) 66–85.
[18] K. Foo, B. Hameed, Insights into the modeling of adsorption isotherm systems, Chem. Eng. J., 156 (2010) 2–10.
[19] Y. Ho, G. McKay, Pseudo-second order model for sorption processes, Process. Biochem., 34 (1999) 451–465.
[20] A. Keränen, T. Leiviskä, O. Hormi, J. Tanskanen, Removal of nitrate by modified pine sawdust: effects of temperature and co-existing anions, J. Environ. Manage., 147 (2015) 46–54.
[21] M. Brebu, C. Vasile, Thermal degradation of lignin: a review, Cell. Chem. Technol., 44 (2010) 353–363.
[22] M. Awalludin, O. Sulaiman, R. Hashim, W. Nadhari, An overview of the oil palm industry in Malaysia and its waste utilization through thermochemical conversion, specifically via liquefaction, Renew. Sustain Energy Rev., 50 (2015) 1469–1484.
[23] X. Xu, B. Gao, X. Tan, Q. Yue, Q. Zhong, Q. Li, Characteristics of amine-crosslinked wheat straw and its adsorption mechanisms for phosphate and chromium (VI) removal from aqueous solution, Carbohydr. Polym., 84 (2011) 1054–1060.
[24] A. Yadav, R. Abbassi, A. Gupta, M. Dadashzadeh, Removal of fluoride from aqueous solution and groundwater by wheat straw, sawdust and activated bagasse carbon of sugarcane, Ecol. Eng., 52 (2013) 211–218.
[25] A. Razaee, H. Godini, S. Dehestani, A. Khavanin, Application of impregnated almond shell activated carbon by zinc and zinc sulfate for nitrate removal from water, Iranian J. Environ. Health Sci. Eng., 5 (2008) 125–130.
[26] C. Namasivayam, D. Sangeetha, Removal of nitrate from water by $ZnCl_2$ activated carbon from coconut coir pith, an agricultural solid waste, Indian J. Chem. Technol., 12 (2005) 513–521.
[27] I. Tsibranska, E. Hristova, Comparison of different kinetic models for adsorption of heavy metals onto activated carbon from apricot stones, Bulgarian Chem. Commun., 43 (2011) 370–377.
[28] Y. Ho, G. McKay, The kinetics of sorption of divalent metal ions onto sphagnum moss peat, Water Res., 34 (2000) 735–742.
[29] A. Bhatnagar, M. Ji, Y. Choi, W. Jung, S. Lee, S. Kim, G. Lee, H. Suk, H. Kim, B. Min, S. Kim, B. Jeon, J. Kang, Removal of nitrate from water by adsorption onto zinc chloride treated activated carbon, Sep. Sci. Technol., 43 (2008) 886–907.
[30] Y. Yu, Y. Zhuang, Z. Wang, Adsorption of water-soluble dye onto functionalized resin, J. Colloid Interface Sci., 242 (2001) 288–293.
[31] R. Katal, M. Baei, H. Rahmati, H. Esfandian, Kinetic, isotherm and thermodynamic study of nitrate adsorption from aqueous solution using modified rice husk, J. Ind. Eng. Chem., 18 (2012) 295–302.
[32] X. Zhang, Y. Shang, L. Wang, Y. Song, R. Han, Y. Li, Comparison of linear and nonlinear regressive analysis in estimating the Thomas model parameters for anionic dye adsorption onto CPB modified peanut husk in fixed-bed column, Adv. Mater. Res., 781–784 (2013) 2179–2183.
[33] X. Xu, B. Gao, Y. Zhao, S. Chen, X. Tan, Q. Yue, J. Lin, Y. Wang, Nitrate removal from aqueous solution by *Arundo donax* L. reed based anion exchange resin, J. Hazard. Mater., 203–204 (2012) 86–92.
[34] S. Chatterjee, D. Lee, M. Lee, S. Woo, Nitrate removal from aqueous solutions by cross-linked chitosan beads conditioned with sodium bisulphate, J. Hazard. Mater., 166 (2009) 508–513.
[35] H. Demiral, G. Gündüzoğlu, Removal of nitrate from aqueous solutions by activated carbon prepared from sugar beet bagasse, Bioresour. Technol., 101 (2010) 1675–1680.